Quantification of Vessel Density in Retinal Optical Coherence Tomography Angiography Images Using Local Fractal Dimension

Santosh G. K. Gadde,[1] Neha Anegondi,[2] Devanshi Bhanushali,[1] Lavanya Chidambara,[1] Naresh Kumar Yadav,[1] Aruj Khurana,[1] and Abhijit Sinha Roy[2]

[1]Retina Department, Narayana Nethralaya Foundation, Bangalore, India
[2]Imaging, Biomechanics and Mathematical Modeling Solutions, Narayana Nethralaya Foundation, Bangalore, India

Correspondence: Abhijit Sinha Roy, Imaging, Biomechanics and Mathematical Modeling Solutions, Narayana Nethralaya, Bangalore, India; asroy27@yahoo.com.

PURPOSE. To evaluate a fully automated local fractal dimension method to quantify vessel density and foveal avascular zone (FAZ) area in optical coherence tomography angiography (OCTA) images.

METHODS. Fifty-two healthy Asian Indian eyes underwent imaging prospectively with OCTA system. Superficial and deep retinal vascular plexus was imaged. Local fractal analysis was applied to the OCTA images. A scan area of 3×3 mm was selected in the superficial and deep retinal layers. Foveal avascular zone area and vessel density were quantified in circular and sectoral zones around the fovea. A unique contour map of vessel density and dropout zones was developed to perform regional comparisons.

RESULTS. Foveal avascular zone of superficial (0.35 ± 0.013 mm^2) and deep (0.49 ± 0.012 mm^2) retinal vascular plexus was segmented. The agreement between the manually segmented and local fractal dimension segmented FAZ area was 0.97 (95% confidence interval [CI]: 0.94–0.98) and did not change significantly with age ($P = 0.94$ and 0.21, respectively). The vessel density was greater in the deep than the superficial retinal vascular plexus ($P < 0.0001$). When the image was subdivided into sectors around the FAZ, inferior sector had greater vessel density than the others (temporal, superior, and nasal) in both superficial and deep retinal vascular plexus ($P < 0.05$). These observations were similar to recent studies on animal retinal vasculature map.

CONCLUSIONS. A novel implementation of local fractal dimension to calculate vessel density and FAZ area was demonstrated. Age did not impact vessel density but sectoral analyses showed greater vessel density in the inferior zone.

Keywords: optical coherence tomography, fractal analysis, angiography, vessel density, fovea

Diagnosis and treatment of diseases that involve vessel abnormalities may require detailed analysis of the retinal vasculature to understand its role in disease pathophysiology.[1–3] Fundus fluorescein angiography (FFA) and indocyanine green angiography (ICGA) are both invasive techniques that require intravenous injection of dye to obtain two dimensional high contrast images of the retinal circulation.[4,5] Confocal scanning laser ophthalmoscopy was developed to provide depth resolved images of the retina[6] but the depth resolution is inadequate to delineate the individual retinal layers and capillaries. Optical coherence tomography angiography (OCTA) is a recent, noninvasive, and dye-less imaging technique for evaluating the vessels by capturing the dynamic motion of the erythrocytes.[7] It has been shown to be a useful imaging modality for evaluation of ophthalmologic diseases, such as AMD, diabetic retinopathy, arteriovenous occlusions, and glaucoma.[8]

A few previous studies on OCTA have been qualitative in nature.[9–12] There have been quantitative studies on the microstructure and microvasculature organization in the human retina using confocal scanning laser microscopy.[13–15] However, more quantitative studies on OCTA are needed.[16]

Therefore, this study was aimed at automated segmentation and quantification of the foveal avascular zone (FAZ) and the vessel density in the superficial and deep retinal vascular plexuses in a healthy population of Asian Indian eyes. This study used local fractal analysis, which quantified the complexity of the vascular network. The method was refined further by using local fractal dimension, which is a technique used to identify local or regional variations in the complexity of an image[17,18] and was used for evaluating the vessel distribution in the OCTA scans. Statistical analysis was performed to assess the distribution of FAZ area and vessel density across different age groups in superficial and deep retinal vascular plexus of healthy subjects.

METHODS

Study Population

This study was approved by the institutional ethics committee of Narayana Nethralaya Multi-Specialty Eye Hospital, Bangalore, India. The research followed the tenets of the Declaration of Helsinki. Written informed consent was obtained from all the subjects before imaging. Fifty-two eyes of healthy Asian Indian

subjects were included in this study. The subjects were between 20 to 67 years of age. Subjects after normal ocular examination with 6/6, N6 vision and refractive error range −1 to +1 diopters (D) were included in the study. Subjects with systemic history of diabetes, hypertension, and other vascular pathologies, refractive error beyond the specified limits, pathologic ocular conditions including glaucoma, inflammatory conditions, history of ocular trauma, and prior ocular surgery were excluded from the study.

Study Design

All subjects underwent imaging on AngioVue OCTA system (Optovue, Inc., Fremont, CA, USA) by a single operator using the AngioVue software of the RTVue XR Avanti Spectral Domain OCT (SD-OCT; Optovue, Inc.). The device has a high acquisition speed of 70,000 A-scans per second. The scan area was 3×3 mm for all the subjects. Analyses were performed on the OCTA images generated from the superficial and deep retinal vascular plexuses.

Study Endpoints

Optical coherence tomography angiography scans of superficial and deep retinal vascular plexuses have a dense vascular network and local fractal dimensions[17,18] were calculated to indicate presence of vessels. Box counting method was used to calculate the fractal dimension given by Equation 1:

$$FractalDimension = \frac{\log(N_s)}{\log(s)}. \qquad (1)$$

In Equation 1, N_s was the number of boxes of magnification (s) needed to enclose the structure. From Equation 1, a moving window of size $(2w + 1) \times (2w - 1)$ was used to calculate the local fractal dimension of the OCTA scans using the following equation[18]:

$$R(i,j) = LocalFractalDimension[I(i + k, j + k); -w < k < w]. \qquad (2)$$

In Equation 2, I was the original image and R was the image formed after replacing the value of center pixel of each window with the fractal dimension of the window.[18] Window sizes (in pixels) of 5×5, 7×7, 9×9, 11×11 and 13×13 were used to calculate the local fractal dimension. Then FAZ was segmented by first binarizing the image followed by connected component labeling (MathWorks, Inc., Natick, MA, USA). The area of FAZ was calculated from the binary image.

Each pixel in the image had a local fractal dimension number, which was calculated using the moving window as described in Equation 2. The fractal dimension value varied with the distribution of vessels around the pixel in the image. Thus, the local fractal dimension of a pixel present in a larger vessel was higher as compared to that of a pixel present in a smaller vessel or in a nonvessel region of the image. The ratio of local fractal dimension of each pixel in an OCTA image to its maximum fractal dimension was calculated. This normalized ratio was then used to plot a contour map. The contour map of the normalized ratio essentially provided a pictorial representation of an apparent probability index of presence of vessel of certain size at each pixel, with an index closer to 1 indicating large vessels and an index closer to 0 indicating nonvessel regions. Figures 1A and 1C show the OCTA image of the superficial and deep retinal vascular plexus of an eye. Figures 1B and 1D show their respective contour maps of the normalized ratio of local fractal dimension at a pixel to maximum value of local fractal dimension in the same image.

By visual examination, the small vessels and capillaries were observed to lie between a ratio value of 0.7 and 0.9. The nonvascular regions were observed to lie between a ratio value of 0.0 and 0.3. The smaller gaps between vessels were observed to lie between a ratio value of 0.3 and 0.7. The larger vessels had the highest magnitude of local fractal dimension and thus, the corresponding pixels within the larger vessels had a normalized ratio close to or equal to 1. Figure 2 shows the contour map of OCTA image of the superficial retinal vascular plexus with the marked FAZ, examples of large and small vessels, along with the gaps between the vessels.

Then vessel density was expressed in percentage by taking the ratio of the total vessel area (all pixels with a ratio value between 0.7 and 1.0) to the total area of analyzed region (size of the image in pixels). Two forms of analyzed regions were used. First vessel density was calculated in three circular regions after excluding the FAZ area from each region, namely, C1 (diameter = 1.5 mm), C2 (diameter = 2 mm) and C3 (diameter = 2.5 mm). Figure 3A shows the OCTA image of a superficial retinal vascular plexus and a schematic representation of the three circular region C1, C2, and C3. Vessel density was also calculated in the parafoveal sectors after excluding the FAZ area from the sectors, namely, temporal (T), superior (S), nasal (N), and inferior (I) sector of a circular zone of diameter 2.5 mm only. Figure 3B shows the OCTA image of a superficial retinal vascular plexus and the schematic four parafoveal sectors (T, S, N, I). All the above methods were implemented using MATLAB v7.10 (Mathworks, Inc.).

Statistical Analysis

All analyzed variables were reported as mean ± SEM after confirming normality of distribution with the Kolmogorov-Smirnov test. The analyzed variables were FAZ area (mm²) and vessel density (%). The agreement between the manual and automated segmentation of FAZ areas for different window sizes was assessed using intraclass correlation coefficient (ICC). Manual segmentation of the FAZ was performed by a single observer using ImageJ software (http://imagej.nih.gov/ij/; provided in the public domain by the National Institutes of Health, Bethesda, MD, USA). The subjects were divided into three age groups: Group A = 20 to 30 years, Group B = 31 to 45 years, and Group C = 46 to 67 years. Repeated measures analysis of variance (rANOVA) was performed among the age groups for each circular zone and sector. A P value less than 0.05 was considered statistically significant. All P values were 2-sided and Bonferroni corrected. All statistical analyses were performed in MedCalc v15.8 (MedCalc, Inc., Ostend, Belgium).

RESULTS

Number of eyes was 17, and 17 and 18 in age groups A, B, and C, respectively. Table 1 shows the ICC between manually segmented FAZ and segmentation of the FAZ using normalized ratio of local fractal dimension. The window size of 5×5 had the best ICC of 0.97 (95% confidence interval [CI]: 0.94-0.98). As the window size was increased, ICC decreased in magnitude. Therefore, only a window size of 5×5 was used for further analyses. The mean area of the FAZ by manual segmentation and segmentation using the normalized ratio in the superficial retinal plexus was 0.36 ± 0.013 mm² and 0.35 ± 0.013 mm², respectively ($P < 0.0001$). Similarly the mean area of FAZ in the deep retinal plexus was 0.49 ± 0.012 mm² and 0.48 ± 0.013 mm², respectively ($P < 0.0001$). The FAZ area in the superficial ($P = 0.94$) and deep retinal vascular ($P =$
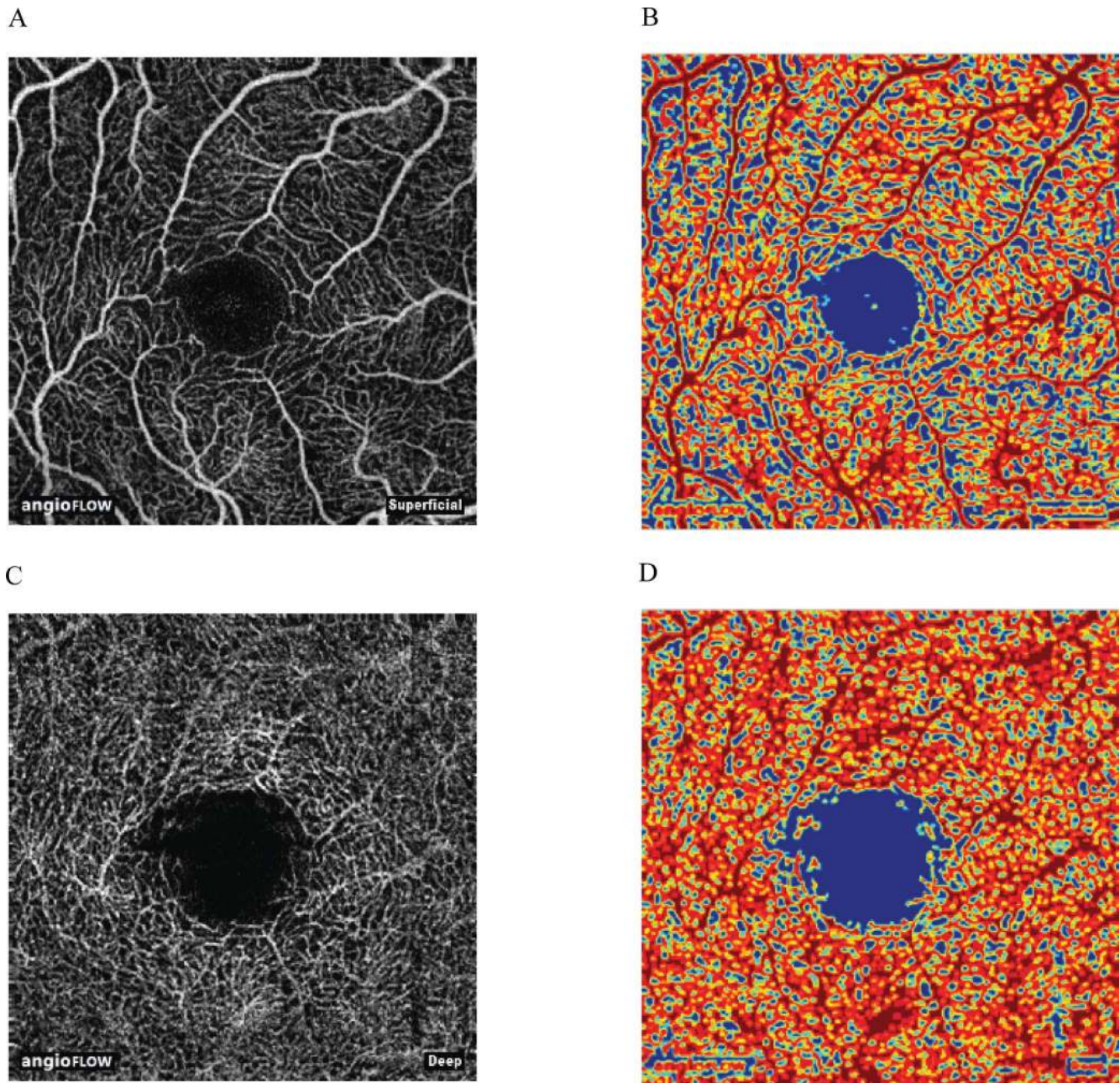
A

B

C

D

FIGURE 1. (A) Optical coherence tomography angiography image of the superficial retinal vascular plexus of size 3×3 mm. (B) Corresponding contour map created with normalized value of local fractal dimension values. (C) Optical coherence tomography angiography image of the deep retinal vascular plexus of size 3×3 mm. (D) Corresponding contour map created with normalized value of local fractal dimension.

0.21) plexus did not change significantly with age of the subject.

Table 2 shows the mean vessel density of the superficial retinal plexus in circular zones (C1, C2, C3) and parafoveal sectors (T, S, N, I) among the age groups. In zones C1, C2, and C3, age did not affect the vessel density ($P = 0.33$, 0.31, and 0.29, respectively). Vessel density in a given age group was similar among the three circular zones ($P > 0.05$). In the parafoveal sectors, the vessel density in the inferior sector was significantly different from the others ($P < 0.001$), for example, in age group A, mean vessel density in the inferior sector (53.61%) was greater than the same in other sectors (48.75% in T, 47.57% in S, and 47.04% in N). However, this difference in vessel density between sectors was independent of age ($P =$

0.92). Table 3 shows the mean vessel density of deep retinal vascular plexus in circular zones (C1, C2, C3) and parafoveal sectors (T, S, N, I) among the age groups. In zones C1, C2 and C3, age did not affect the vessel density ($P = 0.72$, 0.29, and 0.54, respectively). Also, vessel density in a given age group was similar in all circular zones ($P > 0.05$). The vessel density in all the parafoveal sectors was unaffected by age ($P > 0.05$). However, in a given age group, vessel density in superior and inferior sector were similar ($P > 0.05$) but significantly greater than vessel density in the temporal and nasal sector ($P = 0.02$), for example, in age group A, mean vessel density in superior (54.04%) and inferior (56.56%) sector was greater than mean vessel density in temporal (50.44%) and nasal sector (49.68%).
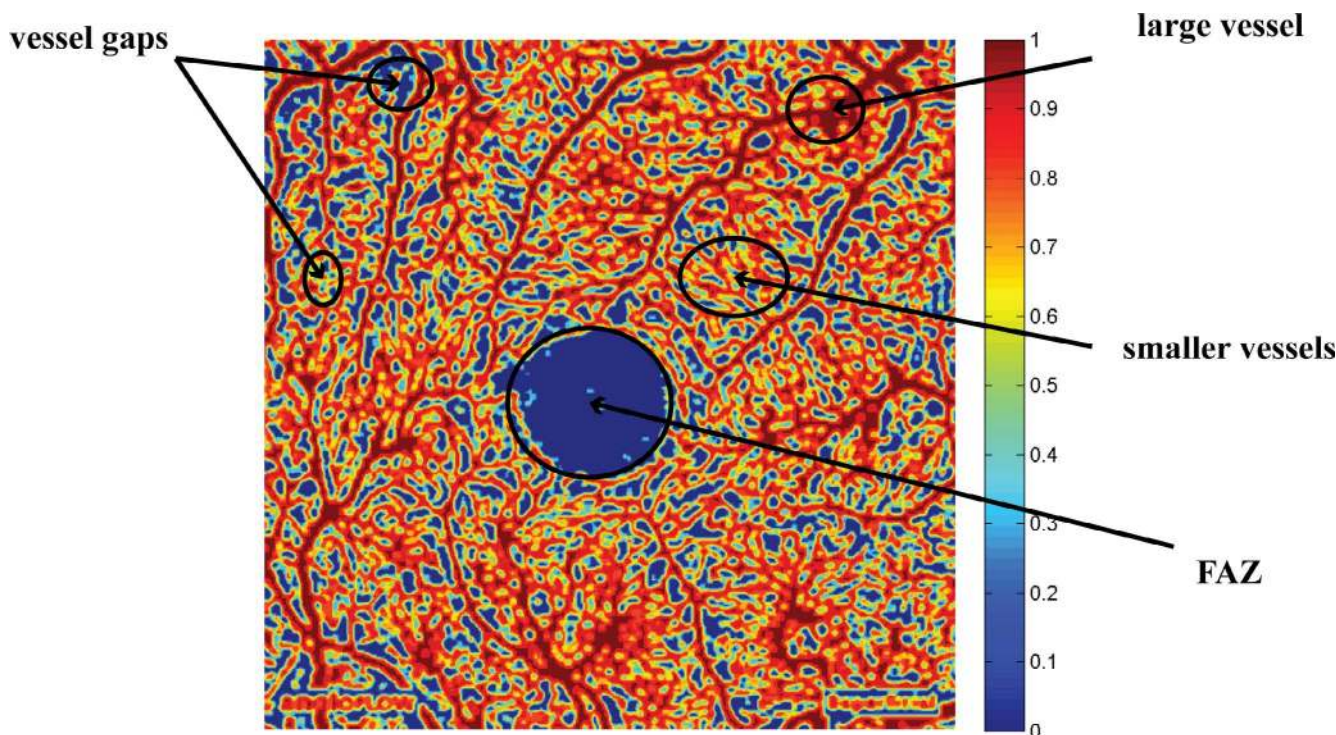
FIGURE 2. Contour map created from OCTA of superficial retinal vascular plexus with marked FAZ, examples of large vessels, small vessels, and vessel gaps.

A bar plot of the observations of the parafoveal sectors from Tables 2 and 3 are plotted in Figures 4A and 4B, respectively.

Because only sector (T, S, N, I)-based analyses achieved statistical analyses independent of age, the proportion of pixels within a range of values of the normalized ratio of local fractal dimension in the superficial and deep (Table 4) retinal vascular plexus of age group A was further analyzed. The proportion of pixels within a range of values of normalized ratio of local fractal dimension was calculated as the ratio of total number of pixels within the range of normalized ratio of local fractal

dimension to the total number of pixels in the image. In the superficial vascular plexus (Table 4), the greater vessel density in the inferior sector was accompanied by reduction in the smaller gaps between the vessels in the same sector relative to others, for example, mean proportion of pixels within range of 0.3 to 0.7 was lower in the inferior sector than the others (I versus S: $P = 0.004$; I versus T: $P = 0.008$; I versus N: $P < 0.0001$). Similarly (Table 4), reduction in the smaller gaps between vessels was found in the inferior sector of the deep retinal vascular plexus compared with its temporal and nasal
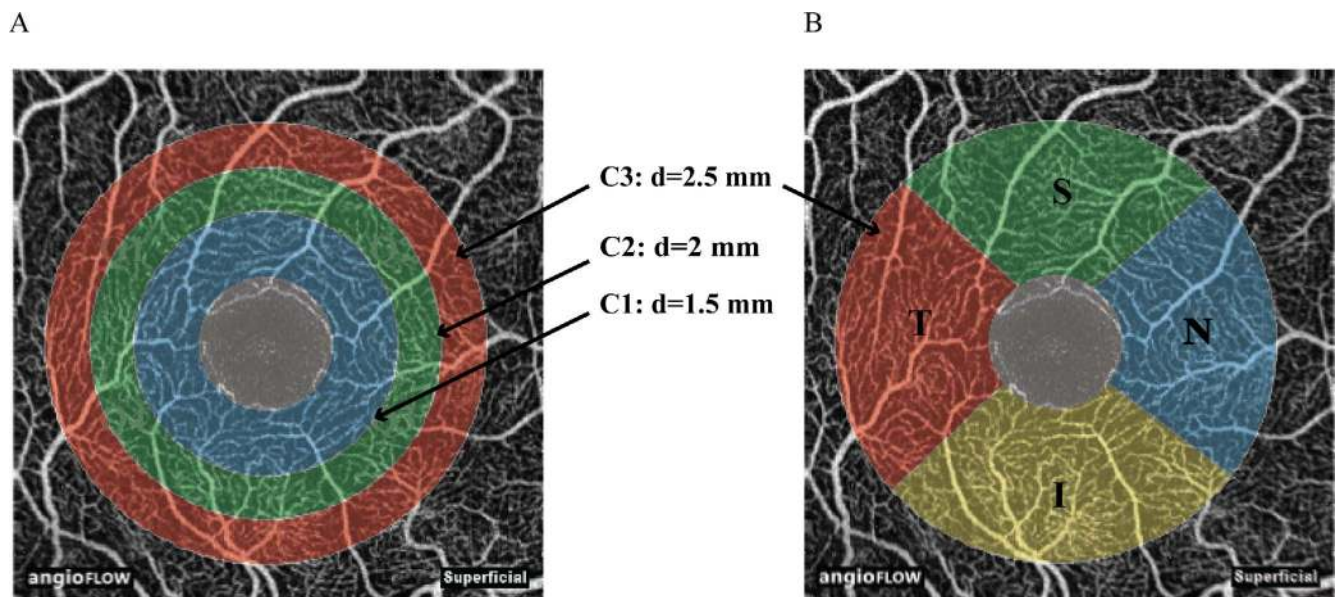

FIGURE 3. (A) Analyses of OCTA of superficial retinal vascular plexus in three circular zones (C1, C2, C3), where d is the diameter. (B) Analyses of OCTA of superficial retinal vascular plexus in four parafoveal sectors: temporal (T), superior (S), nasal (N), and inferior (I).

TABLE 1. Intraclass Correlation Coefficient to Assess Agreement Between Foveal Avascular Area Calculated by Manual Segmentation and Foveal Avascular Area Calculated by Segmentation With the Normalized Ratio of Local Fractal Dimension

Window Size (In Pixels)	ICC	95% CI
5 × 5	0.97	0.94 to 0.98
7 × 7	0.75	0.56 to 0.85
9 × 9	0.55	0.24 to 0.74
11 × 11	0.33	−0.15 to 0.61
13 × 13	0.43	0.01 to 0.66

sector ($P = 0.02$ and 0.001, respectively). The proportion of pixels devoid of any vessels (normalized ratio of local fractal index < 0.3) remained unchanged ($P > 0.05$) among the sectors in both superficial and deep (first column of Table 4) retinal vascular plexus. From all the tabular data, it was evident that vessel density was always lower in the superficial than in the deep retinal vascular plexus ($P < 0.0001$).

DISCUSSION

In this study, local fractal dimension was used for segmenting and quantifying FAZ area and vessel density. The aim of this study was not just the quantification of retinal parameters but also to demonstrate the application and versatility of local fractal dimension in the analyses of OCT angiography images. Fractal objects show details at an arbitrarily small scale and can be used for capturing the complex and detailed microvascular network on OCT angiograms.[17] Because of this complexity, conventional preprocessing techniques related to smoothening or filtering of images were not applied on the OCTA images prior to local fractal dimension calculation as this may have resulted in the loss of smaller vessels and capillaries. Only the motion adjusted (performed by the scanner) OCTA images from the device were analyzed. Fractal analysis has been used previously for measuring the retinal vessel density in fluorescein angiograms and retinal fundus photographs to evaluate the normal and abnormal vascular pattern but the results were inconclusive due to variations in imaging technique and method of fractal analysis used.[19-23] Also, the methods calculated the fractal dimension for the entire image or in fixed regions of the image as compared with the method of

TABLE 2. Mean ± Standard Error of the Vessel Density in Superficial Retinal Vascular Plexus in the Three Circular Zones (Fig. 3A) And Four Sectors (Fig. 3B) Among the Age Groups (A, B, and C) Ranging From 20 to 67 Years

	Vessel Density, %		
	A*	B*	C*
C1†	45.04 ± 1.19	45.19 ± 1.40	49.08 ± 2.99
C2†	47.85 ± 1.26	47.39 ± 1.33	52.10 ± 3.36
C3†	49.19 ± 1.36	48.61 ± 1.21	53.62 ± 3.46
T	48.75 ± 1.41	47.68 ± 1.10	47.98 ± 1.74
S	47.57 ± 1.49	48.39 ± 1.39	47.41 ± 1.19
N	47.04 ± 1.56	47.43 ± 1.29	48.27 ± 1.43
I	53.61 ± 1.57	50.97 ± 1.71	53.61 ± 1.56

Vessel density was defined as the ratio of total number of pixels with normalized ratio of local fractal dimension between 0.7 and 1.0 to the total number of pixels in the image.
* Age groups: A = 20–30, B = 31–45, C = 46–67 years.
† C1 = diameter 1.5, C2 = diameter 2, C3 = diameter 2.5 mm.

TABLE 3. Mean ± Standard Error of the Vessel Density in Deep Retinal Vascular Plexus in the Three Circular Zones (Fig. 3A) and Four Sectors (Fig. 3B) Among the Age Groups (A, B, and C) Ranging From 20 to 67 Years

	Vessel Density, %		
	A*	B*	C*
C1†	48.81 ± 1.46	52.08 ± 2.77	47.21 ± 1.15
C2†	52.78 ± 1.40	56.43 ± 2.47	51.18 ± 1.24
C3†	54.16 ± 1.32	57.83 ± 2.28	52.71 ± 1.13
T	50.44 ± 1.57	54.19 ± 2.32	49.52 ± 1.79
S	54.04 ± 1.29	56.28 ± 2.13	53.77 ± 1.34
N	49.68 ± 1.58	50.47 ± 2.55	50.35 ± 1.66
I	56.56 ± 1.43	57.59 ± 1.94	55.21 ± 1.65

Vessel density was defined as the ratio of total number of pixels with normalized ratio of local fractal dimension between 0.7 and 1.0 to the total number of pixels in the image.
* Age groups: A = 20–30, B = 31–45, C = 46–67 years.
† C1 = diameter 1.5, C2 = diameter 2, C3 = diameter 2.5 mm.
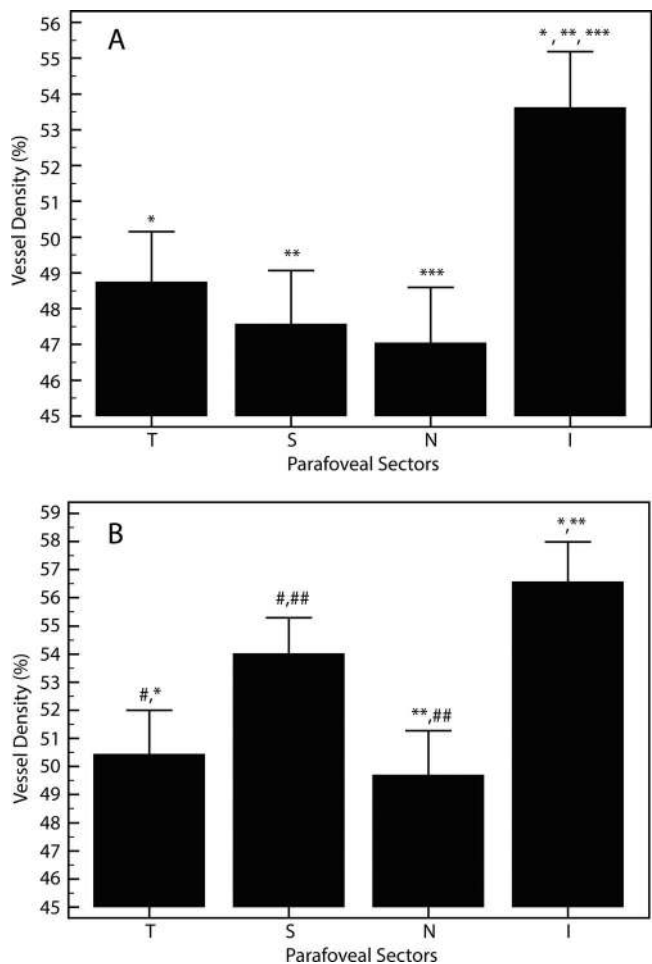

FIGURE 4. (A) Mean vessel density in temporal (T), superior (S), nasal (N), and inferior (I) sectors of the superficial retinal vascular plexus in age group A (20–30 years of age). (B) Mean vessel density in temporal (T), superior (S), nasal (N) and inferior (I) sectors of the deep retinal vascular plexus. *Error bars* show the SEM. *Symbols* indicate statistically significant difference ($P < 0.05$) between the means.

TABLE 4. Mean ± Standard Error of Proportion of Pixels Within a Range of Normalized Ratio of Local Fractal Dimension in the Superficial and Deep Retinal Vascular Plexus of Age Group A

	Proportion, %		
	0.0–0.3	0.3–0.7	0.7–1.0
Superficial retinal vascular plexus			
T	41.64 ± 0.50	9.61 ± 1.53	48.75 ± 1.41
S	42.07 ± 0.67	10.36 ± 1.85	47.57 ± 1.49
N	39.49 ± 0.67	13.47 ± 1.95	47.04 ± 1.56
I	42.52 ± 1.43	3.87 ± 1.27	53.61 ± 1.57
Deep retinal vascular plexus			
T	39.34 ± 0.61	10.22 ± 1.78	50.44 ± 1.57
S	36.98 ± 0.89	9.01 ± 1.61	54.04 ± 1.29
N	37.67 ± 0.52	12.67 ± 1.92	49.68 ± 1.58
I	38.24 ± 0.97	5.21 ± 2.14	56.56 ± 1.43

moving window local fractal dimension used in this study, in order to provide better resolution of the retinal vasculature.

A study on OCTA FAZ area in healthy subjects reported a mean superficial FAZ area equal to 0.358 ± 0.084 mm² and mean deep FAZ area equal to 0.584 ± 0.15 mm (Hsiao Y, et al. *IOVS* 2015;56:ARVO E-Abstract 1646), which were comparable to the results of this study. The FAZ area did not vary significantly with age. Vessel density was similar among the circular zones (C1, C2, and C3 in Fig. 3A). However, the inferior sector had significantly higher vessel density than both temporal and nasal sector with concomitant drop in the gaps between the smaller vessels. This highlights that vessel density analyses in the superficial and deep retinal vascular plexus needs to be a local rather than an average of the whole image. In recent studies on the retina and choroid, the superior, and inferior retinal and choroidal zones were thicker than the nasal and temporal zones.[24,25] This trend is similar to the superficial and deep retinal vascular plexus vessel density mapping across these zones in this study. This indicated a physiological correlation among vessel density, retina, and choroid thickness, which needs to be evaluated further.[26,27] This trend has also been observed in mice in vivo.[24] The study showed that: (1) vessel density in superficial layer (31.49%) was lower than the deeper layer (45.96%),[24] and (2) vessel density was similar among the sectors in the superficial layer but not in the deeper layer.[24] In mice, a small but significant reduction in vessel density was noted in the deep retinal plexus but not in the superficial retinal plexus with age.[24] However, in this study, age did not affect the vessel density in both superficial and deep retinal vascular plexus irrespective of the region (circular or sector) of analyses. In another study on fluorescein angiography of the entire human retina, superior and inferior regions had higher vessel density than nasal temporal,[28] which was similar to the data shown in Figure 4. Further, inferior retina had higher vessel density than the temporal retina by approximately 4%.[28] In this study, the number was approximately 9.9% in both the superficial and deep retinal vascular plexus.

A study on capillary network in the perifovea has demonstrated variation in the capillary density and loop area in different retinal layers, with the deeper layers having larger capillary density and smaller loop area as compared with the superficial layer.[15] These findings[15] were similar to the findings of the current study, where an increase in vessel density and decrease in smaller vessel gaps were shown in the deep retinal vascular plexus as compared with the superficial retinal vascular plexus. Metabolic demands within the retina are heterogeneous and are met by the capillary network, which essentially function to increase the absorption of nutrients and removal of waste. Therefore, it was speculated that the distinct metabolic demands of the superficial and deep retinal vascular plexus may be a reason for the difference in the vessel density in these two layers.[13,15] Similar findings have also been reported in the brain where the microcirculation in the human cerebral cortex is adapted according to the neuronal demands.[29,30] The higher vessel density in the deep retinal vascular plexus may also be attributed to the apparent decrease in the presence of large vessels and relatively denser presence of smaller vessels compared with the superficial layer, which in turn compensates for the lower flow per vessel in the deep retinal vascular plexus.[25]

Optical coherence tomography angiography has a potentially wide applicability in retinal vascular diseases and a study showed that OCT angiograms were similar to fluorescein angiography images in showing important vascular detail.[12] Currently, fluorescein angiography is the gold standard for retinal imaging but it may miss capillary microvasculature information, which may be measured by OCTA due to better resolution. A study also described the characteristics, sensitivity, and specificity of detection of choroidal neovascularization on OCTA, which highlighted the versatility of OCTA in retinal and choroid disease diagnosis.[11] Local fractal analysis can be used to detect such abnormalities in the superficial and deep retinal plexuses as well as in the outer retina and choroid layers. At present, use of OCTA is limited by small field of view unlike fluorescein angiography.[8] However, it provided improved visualization of the radial peripapillary and deep capillary networks, which were not well distinguished in fluorescein angiography in healthy eyes.[7,8] In summary, this study described a novel method for automatic segmentation and quantification of FAZ area and vessel density in superficial and deep retinal vascular plexuses of healthy eyes. Age did not have a significant effect on the FAZ area and vessel density but local analyses of vessel density could be important for evaluation of longitudinal data based on OCTA images of retinal disorders.

References

1. Emre M, Orgul S, Gugleta K, Flammer J. Ocular blood flow alteration in glaucoma is related to systemic vascular dysregulation. *Br J Ophthalmol*. 2004;88:662–666.

2. Wong TY, Klein R, Klein BE, Tielsch JM, Hubbard L, Nieto FJ. Retinal microvascular abnormalities and their relationship with hypertension, cardiovascular disease, and mortality. *Surv Ophthalmol*. 2001;46:59–80.

3. Raja DS, Vasuki S. Automatic detection of blood vessels in retinal images for diabetic retinopathy diagnosis. *Comput Math Methods Med*. 2015;2015:419279.

4. Novotny HR, Alvis D. A method of photographing fluorescence in circulating blood of the human eye. *Tech Doc Rep SAMTDR USAF Sch Aerosp Med*. 1960;60-82:1–4.

5. Landa G, Springer A, Bukelman A, Pollack A. The diagnostic contribution of indocyanine green to fluorescein angiography in fellow drusen eyes of patients with wet age-related macular degeneration. *Eur J Ophthalmol*. 2007;17:615–619.

6. Querques G, Guigui B, Leveziel N, et al. Insights into pathology of cuticular drusen from integrated confocal scanning laser

ophthalmoscopy imaging and corresponding spectral domain optical coherence tomography. *Graefes Arch Clin Exp Ophthalmol*. 2011;249:1617–1625.

7. Spaide RF, Klancnik JM Jr, Cooney MJ. Retinal vascular layers imaged by fluorescein angiography and optical coherence tomography angiography. *JAMA Ophthalmol*. 2015;133:45–50.

8. de Carlo TE, Romano A, Waheed NK, Duker JS. A review of optical coherence tomography angiography (OCTA). *Int J Retin Vitr*. 2015;35:2377–2383.

9. Braaf B, Vienola KV, Sheehy CK, et al. Real-time eye motion correction in phase-resolved OCT angiography with tracking SLO. *Biomed Opt Express*. 2013;4:51–65.

10. Schwartz DM, Fingler J, Kim DY, et al. Phase-variance optical coherence tomography: a technique for noninvasive angiography. *Ophthalmology*. 2014;121:180–187.

11. de Carlo TE, Bonini Filho MA, Chin AT, et al. Spectral-domain optical coherence tomography angiography of choroidal neovascularization. *Ophthalmology*. 2015;122:1228–1238.

12. Matsunaga D, Yi J, Puliafito CA, Kashani AH. OCT angiography in healthy human subjects. *Ophthalmic Surg Lasers Imaging Retina*. 2014;45:510–515.

13. Tan PEZ, Yu PK, Balaratnasingam C, et al. Quantitative confocal imaging of the retinal microvasculature in the human retina. *Invest Ophthalmol Vis Sci*. 2012;53:5728–5736.

14. Yu PK, Balaratsingam C, Cringle SJ, McAllister IL, Provis J, Yu D. Microstructure and network organization of the microvasculature in the human macula. *Invest Ophthalmol Vis Sci*. 2010;51:6735–6743.

15. Chan G, Balaratnasingam C, Yu PK, et al. Quantitative morphometry of perifoveal capillary networks in the human retina. *Invest Ophthalmol Vis Sci*. 2012;53:5502–5514.

16. Jia Y, Bailey ST, Wilson DJ, et al. Quantitative optical coherence tomography angiography of choroidal neovascularization in age-related macular degeneration. *Ophthalmology*. 2013;121:1435–1444.

17. Landini G, Murray PI, Misson GP. Local connected fractal dimensions and lacunarity analyses of 60 degrees fluorescein angiograms. *Invest Ophthalmol Vis Sci*. 1995;36:2749–2755.

18. Taud H, Parrot J-F. Measurement of DEM roughness using the local fractal dimension. *Géomorphologie*. 2005;10:327–338.

19. Avakian A, Kalina RE, Sage EH, et al. Fractal analysis of region-based vascular change in the normal and non-proliferative diabetic retina. *Curr Eye Res*. 2002;24:274–280.

20. Daxer A. The fractal geometry of proliferative diabetic retinopathy: implications for the diagnosis and the process of retinal vasculogenesis. *Curr Eye Res*. 1993;12:1103–1109.

21. Landini G, Misson GP, Murray PI. Fractal analysis of the normal human retinal fluorescein angiogram. *Curr Eye Res*. 1993;12:23–27.

22. Mainster MA. The fractal properties of retinal vessels: embryological and clinical implications. *Eye*. 1990;4(pt 1):235–241.

23. Misson GP, Landini G, Murray PI. Fractals and ophthalmology. *Lancet*. 1992;339:872.

24. McLenachan S, Magno AL, Ramos D, et al. Angiography reveals novel features of the retinal vasculature in healthy and diabetic mice. *Exp Eye Res*. 2015;138:6–21.

25. Savastano MC, Lumbroso B, Rispoli M. In vivo characterization of retinal vascularization morphology using optical coherence tomography angiography. *Retina*. 2015;35:2196–2203.

26. Park KA, Oh SY. Choroidal thickness in healthy children. *Retina*. 2013;33:1971–1976.

27. Huang J, Liu X, Wu Z, Xiao H, Dustin L, Sadda S. Macular thickness measurements in normal eyes with time-domain and Fourier-domain optical coherence tomography. *Retina*. 2009;29:980–987.

28. Pinhas A, Razeen M, Dubow M, et al. Assessment of perfused foveal microvascular density and identification of nonperfused capillaries in healthy and vasculopathic eyes. *Invest Ophthalmol Vis Sci*. 2014;55:8056–8066.

29. Craigie EH. The vascularity of the cerebral cortex of the albino rat. *J Comp Neurol*. 1921;33:193–212.

30. Motti ED, Imhof HG, Yasargil MG. The terminal vascular bed in the superficial cortex of the rat. An SEM study of corrosion casts. *J Neurosurg*. 1989;65:834–846.